

DT Fusion Ignition of LHD-Type Helical Reactor by Joule Heating Associated with Magnetic Axis Shift^{*})

Tsuguhiro WATANABE

National Institute for Fusion Science, 322-6 Oroshi-cho, Toki 509-5292, Japan

(Received 6 December 2010 / Accepted 30 June 2011)

A new concept to achieve current drive with magnetic axis shift, which is caused by vertical magnetic field coil current change in LHD-type magnetic configuration, is proposed. It is confirmed numerically that an LHD-type helical fusion reactor can be ignited by high-current Joule heating. MHD stability of the plasma current in a helical system is analyzed theoretically. Large plasma current that flows in the opposite direction of the helical coil current is MHD stable. Currents with a hollow current profile are more stable than those with a flat-top profile. The central peak current profile will be redistributed to the hollow current profile. A new concept involving the current-driven and current-less hybrid operational scenario of an LHD-type helical reactor is discussed.

© 2011 The Japan Society of Plasma Science and Nuclear Fusion Research

Keywords: LHD, fusion reactor, Joule heating, high beta, MHD stability

DOI: 10.1585/pfr.6.2405130

1. Introduction

LHD-type magnetic configuration (Heliotron configuration) is produced by continuous helical and vertical coil systems. LHD experiments have achieved an average beta value of 5% without beta collapse.

Pressure-driven toroidal current (bootstrap current) cancels the magnetic field in the outer region of the helical coils and reduces the MHD potential energy depending on the plasma beta values. The reduction of the MHD potential energy leads to MHD stability of the LHD plasma [1]. This stability mechanism suggests the possibility of Joule heating of the LHD plasma by large toroidal plasma current that flows opposite to the helical coil current.

The confinement of the ohmically heated $\ell = 2$ stellarator plasma was experimentally studied in the JIPP T-II [2, 3]. No major disruptions were observed when the rotational transform angle due to helical field $t_h/2\pi$ was larger than 0.14 ($I_p \gtrsim 100$ kA at $B_t = 2.2$ T) [2]. In addition, no positional disturbances were well confirmed by the experimental results [3]. Joule heating of the heliotron plasma was carried out in Heliotron DR. Ohmic heating coils were installed in Heliotron DR. The experiment proved that the Joule heating method is a good candidate for providing high-density target plasma. This method requires no extra major equipment (coils, antennas or power supplies) [4].

However, Joule heating power diminishes as $T_e^{-3/2}$ because of the high conductivity of high temperature plasma. Then, powerful external sources of plasma heating are required in the typical modern fusion experimental devices.

When large plasma current is MHD stable, high conductivity of the plasma becomes favorable for Joule heat-

ing of the plasma, because the one-turn voltage necessary for the current drive is significantly reduced. A helical magnetic system can initially prepare the high-temperature and high-density plasma, because a vacuum magnetic surface exist. Then, sufficient toroidal current can be driven by slowly increasing the poloidal magnetic flux.

In Sec. 2, we describe the current drive mechanism that couples with the real time shift of the magnetic axis. In Sec. 3, we describe the theoretical model for the current drive of the plasma. We show numerically that Joule heating coupled with the magnetic axis shift ignites the DT fusion reactor. In Sec. 4, the MHD stability of the large plasma current is discussed. In Sec. 5, we discuss our results.

2. Current Drive by Magnetic Axis Shift

The LHD coil system is composed of a helical coil system and a vertical coil system. Current in the vertical coils can control the characteristics of the magnetic surface. Here, we analyze the magnetic system shown in Fig. 1, which shows an similar extension of the LHD configuration. The shapes of the helical coils are modified to obtain sufficient blanket space for the DT reactor. The IV coil is also modified from the shape of the LHD IV coil to obtain the sufficient magnetic flux change for the plasma current drive. The IV coil serves as the central solenoid coils of a tokamak reactor for the current drive. The currents of the HC, OV, and IS coils shown in Fig. 1 are assumed to be supplied by constant current sources with current values that optimize the magnetic surface ($B_{ax} = 5$ T: magnetic axis position is "C" in Fig. 1). IV coil current $I_{V_{cur}}(t)$ is varied to shift the position of the magnetic axis

author's e-mail: wata@toki-fs.jp

^{*}) This article is based on the presentation at the 20th International Toki Conference (ITC20).

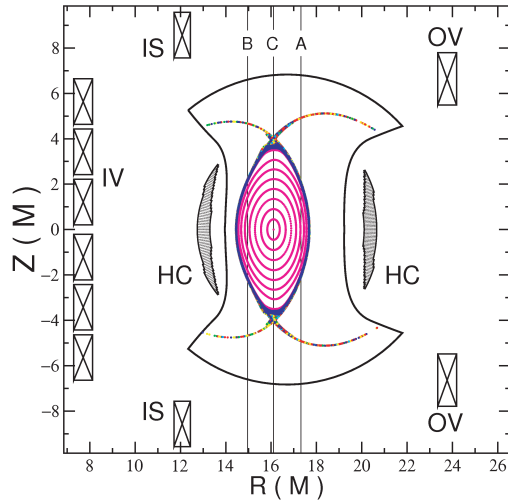


Fig. 1 An example of coil systems and machine size for a DT reactor. A Poincaré plot of the lines of force for an optimized magnetic surface, similarity expanded vacuum vessel of the LHD, cross sections of the helical coils (HC) and the vertical field coils (IV, IS, OV) are shown. The position of the magnetic axis can be shifted from “A” to “C” by the IV coil current.

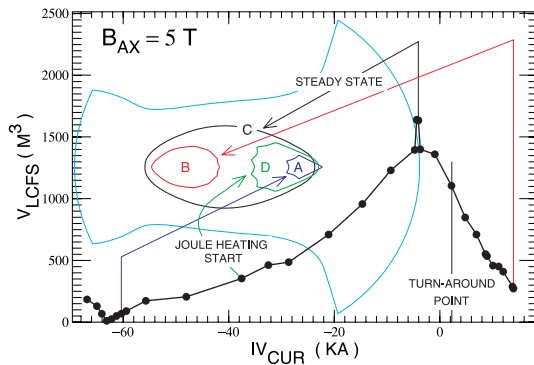


Fig. 2 Variation of the volume and shape of the last closed magnetic surface with the IV coil (2880 turns) current sweep. The magnetic surface “D” is the initial magnetic surface before Joule heating. The magnetic surface “C” is the steady-state magnetic surface after terminating Joule heating. The turn-around point of the IV coil current is also shown.

as shown in Fig. 2.

When the IV coil current is significantly reduced, the magnetic axis moves to the outer shift position, as shown by area “A” in Fig. 2. In contrast, when the IV coil current is significantly increased, the magnetic axis moves to the inner shift position as shown by area “B” in Fig. 2.

The ramp-up of the IV coil current produces the toroidal one-turn voltage necessary for the plasma toroidal current, similar to the vertical field current drive in a tokamak. Because the high-temperature and high-density plasma can be prepared in the magnetic surface region before the current ramp-up, slow ramp-up (with a typical time

constant of the order of 100 s) of the IV coil current is sufficient to ignite the fusion reactor.

3. Model for Current Drive and DT Fusion Ignition by Joule Heating

We analyzed the plasma Joule heating method by examining the coupling systems for the IV coil current equation (1), the plasma loop current equation (2), and the plasma power balance equation (3):

$$V_c = R_c i_c + L_c \frac{di_c}{dt} + \alpha \sqrt{L_p L_c} \frac{di_p}{dt}, \quad (1)$$

$$0 = R_p i_p + L_p \frac{di_p}{dt} + \alpha \sqrt{L_p L_c} \frac{di_c}{dt}, \quad (2)$$

$$\frac{d}{dt} (3nTV_{\text{lcf}s}) = -\frac{3nTV_{\text{lcf}s}}{\tau_E} - P_{\text{BRM}} + R_p I_p^2 + P_{\text{ECH}} + P_F, \quad (3)$$

where, i_c , i_p , and T are the IV coil current, plasma current, and plasma temperature, respectively. The plasma density is assumed to be sustained constant.

Resistance R_c inserted in the IV coil circuit was set so that the time constant of the IV coil current was 100 s. Self inductance of the IV coil group L_c was assumed to be the following value from the geometrical shape and the total turn number (= 2880 turns):

$$R_c/L_c = 100, \quad L_c = 796.5 \text{ H}. \quad (4)$$

The self-inductance and loop resistance of the plasma torus were calculated assuming a circular cross section with minor radius a_p and major radius R_{ax} :

$$L_p = \mu_0 R_{\text{ax}} \left[\ln \left(\frac{8R_{\text{ax}}}{a_p} \right) - \frac{7}{4} \right], \quad 2\pi^2 a_p^2 R_{\text{ax}} = V_{\text{lcf}s}, \quad (5)$$

$$R_p = \frac{2\pi R_{\text{ax}}}{\pi a_p^2} 1.65 \times 10^{-9} Z_{\text{eff}} T [(keV)]^{-3/2} \ln \Lambda. \quad (6)$$

Coupling constant α between the plasma loop and the IV coil was assumed to be 0.3 because of the average radius ratio $R_{\text{IV}}/R_{\text{ax}} \approx 0.48$.

$$\ln \Lambda = 15.5 + \ln \frac{T [(keV)]}{n/10^{20}}, \quad (7)$$

$$P_{\text{BRM}} = 5.4 \times 10^3 Z_{\text{eff}} (n/10^{20})^2 \sqrt{T [(keV)]} V_{\text{lcf}s}. \quad (8)$$

P_{BRM} , P_F , and P_{ECH} are the Bremsstrahlung loss, alpha heating ratio, and ECH heating power, respectively.

We assume $Z_{\text{eff}} = 2$ and energy confinement time τ_E for the current-carrying helical systems as a hybrid combination of τ^{ISS95} [5] and $\tau^{IPB98y2}$ [6] given by

$$\frac{1}{\tau_E} = \frac{1}{\gamma_{\text{iss}} \tau^{ISS95}} \cdot \frac{I_0^2}{I_0^2 + I_p^2} + \frac{1}{\tau^{IPB98y2}} \cdot \frac{I_p^2}{I_0^2 + I_p^2}, \quad (9)$$

where γ_{iss} represents the confinement enhancement factor over the ISS95 scaling; it is assumed to be $\gamma_{\text{iss}} = 2.3$ in the following computations. I_0 is a constant parameter of

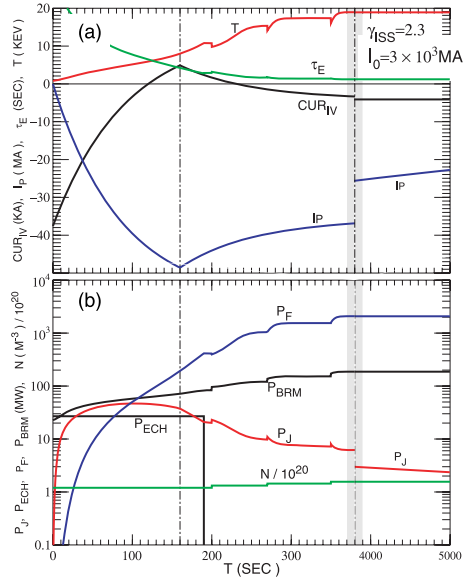


Fig. 3 (a) Time evolution of the IV coil current IV_{cur} , plasma temperature T , plasma current I_p , and energy confinement time τ_E . (b) Time evolution of Joule heating power P_J , alpha heating power P_F , ECH heating power P_{ECH} , Bremsstrahlung loss P_{BRM} , and electron density N . At $t = 160$ s, applied voltage for the IV coil was switched to the value for the optimized magnetic surface “C” in Fig. 2. At $t = 200, 270$, and 350 s, the plasma density was increased by pellet injection so that the fusion power was 2 GW at steady-state operation.

Table 1 Parameters for the initial and stationary states.

t (s)	0	∞
N (m^{-3})	1.2×10^{20}	1.56×10^{20}
T (keV)	0.8	18.9
β (%)	0.31	9.50
P_{BRM} (MW)	22.72	186.68
P_{ECH} (MW)	26.92	0
P_F (GW)	0.367×10^{-5}	2.077

Table 2 Parameters at the time of maximum Joule heating.

t (sec)	I_p (MA)	P_J (MW)	P_{BRM} (MW)	P_F (MW)
102.31	40.02	46.85	58.18	53.166

the fitting. When $I_p \ll (\gg) I_0$, the energy confinement is essentially governed by the ISS95 (IPB98y2) scaling.

Applied voltage for the IV coil V_c was set to obtain the optimized magnetic surface “C” in the steady state starting from magnetic surface “D” in Fig. 2. To obtain sufficient magnetic flux change for the current drive, voltage slightly in excess was applied for a short time ($t \leq 150$ s). The numerical results with $I_0 = 3 \times 10^3$ MA ($\gg I_p$) are shown in Fig. 3. The parameters just before Joule heating starts (initial) and for the stationary state are summarized in Table 1. The parameters at the time of maximum Joule heating are summarized at Table 2.

4. MHD Stability of Plasma Current

The symmetry of an LHD-type magnetic field with helical pitch p can be manipulated using rotating helical coordinate system (X, Y, ϕ) [1, 7]. Two independent conserved quantities Ψ and I derived from MHD equation, $\nabla P = \mathbf{J} \times \mathbf{B}$,

$$0 = \mathbf{B} \cdot \nabla P \implies 0 = \delta \int \mathbf{A} \cdot d\mathbf{x}, \quad (10)$$

and

$$0 = \mathbf{J} \cdot \nabla P \implies 0 = \delta \int \mathbf{B} \cdot d\mathbf{x}, \quad (11)$$

are expressed by the adiabatic invariance

$$\Psi = \frac{1}{2\pi} \oint \left\{ r A_\phi + p(-Y A_X + X A_Y) \right\} d\phi, \quad (12)$$

$$I(\Psi) = \frac{1}{2\pi} \oint \frac{2\pi}{\mu_0} \left\{ r B_\phi + p(-Y B_X + X B_Y) \right\} d\phi, \quad (13)$$

where $I(\Psi)$ represents the driven current term and $P = P(\Psi)$. Plasma current \mathbf{J} is given by

$$\mathbf{J} = \frac{I'(\Psi)}{2\pi} \mathbf{B} + P'(\Psi) \left[\frac{\mathbf{B} \times \nabla \Psi}{|\mathbf{B}|^2} + \alpha(\mathbf{x}) \mathbf{B} \right], \quad (14)$$

where $\alpha(\mathbf{x})$ is given by condition $\nabla \cdot \mathbf{J} = 0$ as

$$\alpha(\mathbf{x}) = - \int d\ell \frac{1}{|\mathbf{B}|} \nabla \cdot \left(\frac{\mathbf{B} \times \nabla \Psi}{|\mathbf{B}|^2} \right), \quad (15)$$

where $d\ell$ expresses the integration along the lines of force. Magnetic field \mathbf{B} and vector potential \mathbf{A} are calculated from the coil current and the plasma current by using the Biot-Savart law. Equilibrium can be calculated from the relaxation scheme.

The plasma stability is determined by the MHD potential energy [8]:

$$W = \int dV \left(\frac{3}{2} P + \frac{1}{2\mu_0} \mathbf{B}^2 \right) \equiv W_T + W_B. \quad (16)$$

W minimum configuration is an MHD-stable equilibrium. When $\delta W < 0$ ($\delta W = W - W_0$, $W_0 \equiv \int dV \frac{1}{2\mu_0} \mathbf{B}_{\text{ext}}^2$), transition to the vacuum state is energetically prohibited. Beta collapse of the core plasma does not occur.

Next, we use the straight helical model and introduce rotating helical coordinate system (X, Y, ζ) [9], which rotates in synchronization with the helical coils. ζ is the axial coordinate. In this case, equations (12) and (14) can be expressed analytically:

$$\Psi = A_\zeta + k(XA_Y - YA_X), \quad (17)$$

$$\mathbf{J} = \frac{1}{\mu_0} I'(\Psi) \mathbf{B} + P'(\Psi) \begin{pmatrix} -kY \\ kX \\ 1 \end{pmatrix}, \quad (18)$$

where k is the axial wave number of the helical coils and determines the helical pitch parameter $\gamma \equiv k \times a_c$ (a_c is

the radius of the helical coil current center). In the following, we have assumed pressure to have a flat-top profile by using the value of the flux function at separatrix Ψ_s :

$$P(\Psi) = \beta_{ax} \frac{B_{ax}^2}{2\mu_0} \exp \left\{ -7 \left(\frac{\Psi}{\Psi_s} \right)^2 \right\}. \quad (19)$$

The driven current is assumed to have a central peak profile or a hollow profile:

$$I'(\Psi) = I_0 \exp \left\{ -7 \left(\frac{\Psi}{\Psi_s} \right)^2 \right\} \text{ (central peak), and} \quad (20)$$

$$= -I_0 \frac{\Psi}{\Psi_s} \exp \left\{ -7 \left(\frac{\Psi}{\Psi_s} \right)^2 \right\} \text{ (hollow).} \quad (21)$$

Numerical results are shown in Fig. 4 for the case of $\gamma = 1.1221$ and $\beta_{ax} = 20\%$.

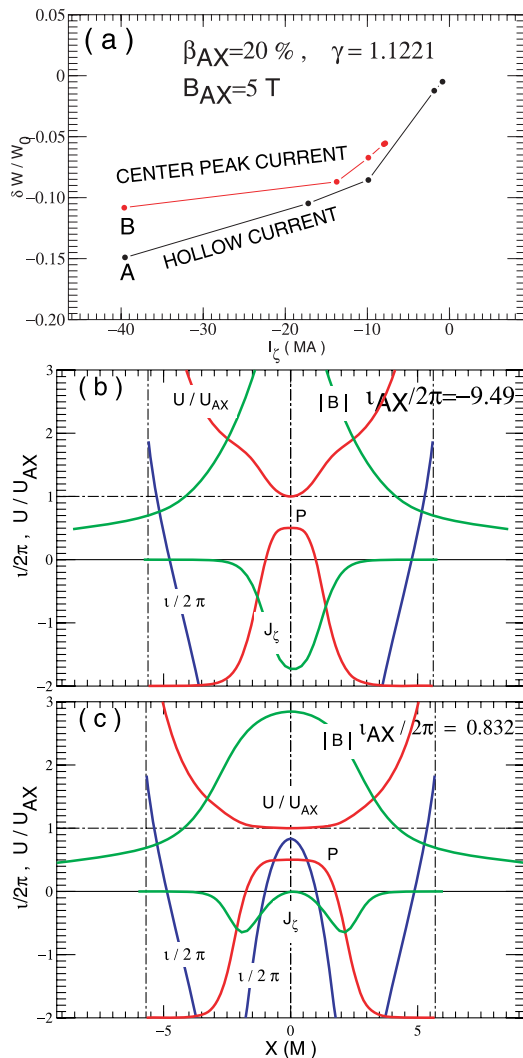


Fig. 4 (a) Variation of MHD potential energy δW as a function of driven plasma current I_ζ for the cases of central peak and hollow current profiles. (b) and (c) show pressure, magnetic field intensity, specific volume and rotational transform corresponding to plasma current A and B, respectively, as labeled in (a).

Figure 4(a) shows that the large positive driven current destabilizes the equilibrium. In contrast, the driven current that flows opposite to the helical coil current shows a tendency to stabilize the equilibrium, and is expected to be disruption free ($\delta W < 0$). However, because of the paramagnetic property of the central peak current, the magnetic hill becomes extensively large, as shown in Fig. 4(b). Then, the central peak current profile will be redistributed to the hollow current profile shown in Fig. 4(c), which is stabilized by strong magnetic shear.

5. Discussion

We proposed a new concept for achieving current drive with the magnetic axis shift. In addition to Joule heating, the plasma current also improves the plasma confinement performance as shown in the IPB98y2 scaling [6]. This leads to a possibility of “current-driven and current-less” hybrid operational scenario for an LHD-type helical reactor. Fusion ignition of a low-density current carrying plasma is relatively easy because of a high confinement performance. Strong alpha heating after the ignition enables the transfer to a steady-state burning of high-density plasma in current-less mode. To confirm the “current-driven and current-less” hybrid operational scenario for an LHD-type helical reactor, we have calculated the equations (1)-(9) with $I_0 = 3$ MA. A numerical result is shown in Fig. 5. The confinement improvement achieved using large plasma current is interesting for future research although in this work we adopted a model for the energy confinement time eq. (9).

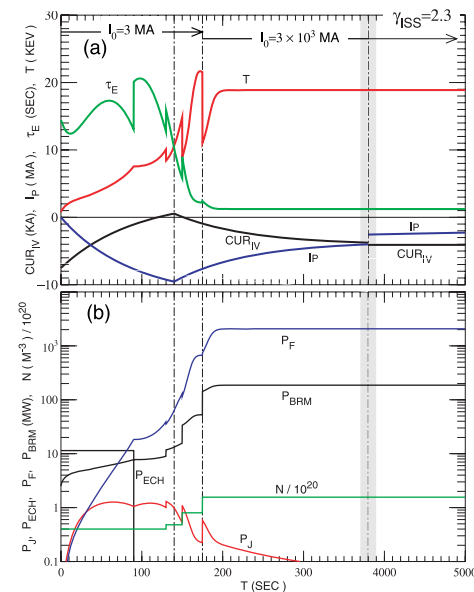


Fig. 5 Current-driven and current-less hybrid operational scenario for an LHD-type helical reactor. To confirm steady-state burning of the current-less plasma in short computational time, I_0 is artificially set equal to 3×10^3 MA after $t > 175$ s.

For discussing the current drive in helical systems, the author thanks the members of the Meeting on Helical Reactor Design at the National Institute for Fusion Science. The author expresses gratitude to the Prof. Nagato Yanagi for detailed discussions on the Joule heating experiments with the Heliotron DR. The author also thanks the referee for the concept of the “current-driven and current-less hybrid operational scenario of an LHD-type helical reactor”. This work was performed with the support and under the auspices of the NIFS Collaborative Research Programs NIFS10KDBF001, NIFS09KTBL010 and NIFS10KNXN195.

- [1] T. Watanabe and A. Sagara, *J. Plasma Fusion Res. SERIES* **9**, 118 (2010).
- [2] J. Fujita *et al.*, *IEEE Trans. Plasma Sci.* **9**, 180 (1981).
- [3] K. Sakurai *et al.*, *J. Phys. Soc. Jpn.* **49**, 759 (1980).
- [4] S. Morimoto *et al.*, *Jpn. J. Appl. Phys.* **25**, 1445 (1986).
- [5] U. Stroth *et al.*, *Nucl. Fusion* **36**, 1063 (1996).
- [6] ITER Physics Basis Editors *et al.*, *Nucl. Fusion* **39**, 2137 (1999).
- [7] T. Watanabe *et al.*, *Nucl. Fusion* **46**, 291 (2006).
- [8] G. Bateman, *MHD Instabilities*, (MIT Press, Cambridge, Massachusetts, and London, England, 1980) p.38.
- [9] T. Watanabe and H. Hojo, *Plasma Fusion Res.* **5**, S2022 (2010).